

BT7480, a novel fully synthetic *Bicycle* tumor-targeted immune cell agonist™ (*Bicycle* TICA™) induces tumor localized CD137 agonism

Kristen Hurov,¹ Johanna Lahdenranta,¹ Punit Upadhyaya,¹ Eric Haines,¹ Heather Cohen,¹ Elizabeth Repash,¹ Drasti Kanakia,¹ Jun Ma,¹ Julia Kristensson,² Fanglei You,¹ Carly Campbell,¹ David Witty,² Mike Kelly,² Stephen Blakemore,¹ Phil Jeffrey,² Kevin McDonnell,¹ Philip Brandish,¹ Nicholas Keen ¹

To cite: Hurov K, Lahdenranta J, Upadhyaya P, *et al.* BT7480, a novel fully synthetic *Bicycle* tumor-targeted immune cell agonist™ (*Bicycle* TICA™) induces tumor localized CD137 agonism. *Journal for ImmunoTherapy of Cancer* 2021;**9**:e002883. doi:10.1136/jitc-2021-002883

► Additional supplemental material is published online only. To view, please visit the journal online (<http://dx.doi.org/10.1136/jitc-2021-002883>).

KH and JL contributed equally.

Accepted 01 October 2021



© Author(s) (or their employer(s)) 2021. Re-use permitted under CC BY-NC. No commercial re-use. See rights and permissions. Published by BMJ.

¹Bicycle Therapeutics, 4 Hartwell Place, Lexington, Massachusetts, USA

²Bicycle Therapeutics, B900 Building, Babraham Research Campus, UK

Correspondence to

Dr Nicholas Keen;
nicholas.keen@bicyclttx.com

ABSTRACT

Background CD137 (4-1BB) is an immune costimulatory receptor with high therapeutic potential in cancer. We are creating tumor target-dependent CD137 agonists using a novel chemical approach based on fully synthetic constrained bicyclic peptide (*Bicycle*®) technology. Nectin-4 is overexpressed in multiple human cancers that may benefit from CD137 agonism. To this end, we have developed BT7480, a novel, first-in-class, Nectin-4/CD137 *Bicycle* tumor-targeted immune cell agonist™ (*Bicycle* TICA™).

Methods Nectin-4 and CD137 co-expression analyses in primary human cancer samples was performed. Chemical conjugation of two CD137 *Bicycles* to a Nectin-4 *Bicycle* led to BT7480, which was then evaluated using a suite of in vitro and in vivo assays to characterize its pharmacology and mechanism of action.

Results Transcriptional profiling revealed that Nectin-4 and CD137 were co-expressed in a variety of human cancers with high unmet need and spatial proteomic imaging found CD137-expressing immune cells were deeply penetrant within the tumor near Nectin-4-expressing cancer cells. BT7480 binds potently, specifically, and simultaneously to Nectin-4 and CD137. In co-cultures of human peripheral blood mononuclear cells and tumor cells, this co-ligation causes robust Nectin-4-dependent CD137 agonism that is more potent than an anti-CD137 antibody agonist. Treatment of immunocompetent mice bearing Nectin-4-expressing tumors with BT7480 elicited a profound reprogramming of the tumor immune microenvironment including an early and rapid myeloid cell activation that precedes T cell infiltration and upregulation of cytotoxicity-related genes. BT7480 induces complete tumor regressions and resistance to tumor re-challenge. Importantly, antitumor activity is not dependent on continuous high drug levels in the plasma since a once weekly dosing cycle provides maximum antitumor activity despite minimal drug remaining in the plasma after day 2. BT7480 appears well tolerated in both rats and non-human primates at doses far greater than those expected to be clinically relevant, including absence of the hepatic toxicity observed with non-targeted CD137 agonists.

Conclusion BT7480 is a highly potent Nectin-4-dependent CD137 agonist that produces complete regressions and antitumor immunity with only intermittent drug exposure in syngeneic mouse tumor models and is well tolerated in preclinical safety species. This work supports the clinical investigation of BT7480 for the treatment of cancer in humans.

BACKGROUND

CD137 (4-1BB/TNFRSF9) is an inducible costimulatory receptor belonging to the tumor necrosis factor (TNF) receptor superfamily involved in the activation of T cells, natural killer (NK) cells, and other immune cells.^{1–3} Based on a strong mechanistic rationale and robust preclinical proof of concept,^{4,5} CD137 has been recognized for its potential as a promising target in cancer, but this promise has not been realized for patients due to hepatic toxicity and limited efficacy observed in the initial therapies evaluated, including the agonistic CD137 antibodies, urelumab and utomilumab.^{6–8} Thus, alternative approaches to modulate this important target are warranted. More recent strategies are focused on bispecific approaches aimed at promoting tumor-target mediated clustering of CD137 to limit systemic and liver toxicities^{9–11} and early patient data shows encouraging evidence of safety and clinical benefit with correlative pharmacodynamics.^{12,13}

We recently reported that fully synthetic bicyclic peptides (*Bicycles*), discovered via phage display and optimized using structure-driven design and medicinal chemistry, can be used as building blocks to create novel synthetic immune agonists. These *Bicycle* tumor-targeted immune cell agonists (*Bicycle* TICAs) could achieve clustering and activation of CD137 using a highly expressed tumor

antigen to provide a scaffolding function to oligomerize the CD137 *Bicycle* presented to immune cells.¹⁴

Nectin-4 (also known as PVRL4) is an epithelial cell adhesion molecule from the nectin and nectin-like family which interact through their extracellular domains to support cell–cell adhesion and are integral to the formation of both homotypic and heterotypic cell junctions.¹⁵ Nectin-4 is highly expressed on multiple human cancers, including bladder, breast, lung, and head and neck cancers^{16–18} and elevated Nectin-4 expression in tumors has been correlated with poor prognosis in pancreatic, breast, gastric, and esophageal cancers.^{17 19–21} A Nectin-4 targeted antibody drug conjugate enfortumab vedotin (EV) that directs the highly potent microtubule-disrupting agent MMAE (monomethyl auristatin E) to tumors has shown high response rates in bladder cancer, providing validation for Nectin-4 as a tumor target.²² Furthermore, combination of EV with checkpoint inhibitor therapy has highlighted the opportunity for immunotherapy in Nectin-4 positive malignancies.²³ Also, tumor indications that are insensitive to or that have become resistant to the MMAE payload may benefit from CD137 agonism.

Here we describe BT7480, a Nectin-4/CD137 *Bicycle* TICA, as the first of this class of compounds to advance through preclinical development for the treatment of patients with Nectin-4 expressing solid tumors.

METHODS

Cell lines and reagents

HT-1376, T-47D, 4T1, NCI-H322, A549 and CT26 cells were obtained from ATCC (American Type Culture Collection). MC38 cells were obtained from the National Cancer Institute (L-159-2018/1). 4T1, CT26 and MC38 cells were engineered to express mouse Nectin-4 (NM_027893.3) as described.¹⁴ Human peripheral blood mononuclear cell (PBMC) isolation was described.¹⁴

Anti-CD137 antibody agonist was purchased from Creative Biolabs (anti-human 4-1BB therapeutic antibody, urelumab, Cat. No. TAB-179).

Recombinant proteins: Human proteins. CD137 (92 204B, R&D Systems), OX40 (OX0-H5224, ACROBiosystems), CD40 (CD0-H5228, ACROBiosystems), Nectin-1 (2880-N1, R&D Systems), Nectin-2 (2229-N2, R&D Systems), Nectin-3 (3064-N3, R&D Systems), Nectin-like-1 (3678-S4-050, R&D Systems), Nectin-like-2 (3519-S4-050, R&D Systems), Nectin-like-3 (4290-S4-050, R&D Systems), Nectin-like-4 (4164-S4, R&D Systems) and Nectin-like-5 (2530-CD-050, R&D Systems). **Mouse proteins.** CD137 (41B-M52H7, ACROBiosystems) and Nectin-4 (3116-N4, R&D Systems). **Rat proteins.** CD137-Fc (R&D Systems, 7968-4B). **Cynomolgus monkey proteins.** CD137 (ACROBiosystems, 41B-C52H4). Human, rat and cyno Nectin-4 cloning, expression, and purification are described in the online supplemental materials.

Methods for synthesis and purification of the molecules can be found in the online supplemental materials.

TCGA data analysis

RNA sequencing data for Nectin-4 (PVRL4) and CD137 (TNFRSF9) from 12,564 tumor samples across 36 cancers were downloaded from The Cancer Genome Atlas Network Genomic Data Commons (TCGA GDC) portal (<http://portal.gdc.cancer.gov>) using FirebrowseR. Methods for expression analysis can be found in the online supplemental materials.

MultiOmyx™ hyperplexed immunofluorescence assay

MultiOmyx™ was performed at NeoGenomics to evaluate the expression of Nectin-4, CD137, CD19, CD3, CD4, CD8, CD56, CD68, and PanCK in 15 human tumor FFPE (Formalin-Fixed Paraffin-Embedded) samples including head and neck squamous carcinoma (HNSCC), non-small cell lung cancer (NSCLC), and bladder cancer. Detailed methods for the MultiOmyx™ assay can be found in the online supplemental materials.

In vitro binding and bioactivity assays

Methods for the CD137 reporter assay, cytokine release assays with cytokine quantification, and cell receptor quantification (qFlow) have been described¹⁴ in detail. Methods for the CD137L binding competition assay and surface plasmon resonance binding assays can be found in the online supplemental materials. Retrogenix's cell microarray technology²⁴ was used to screen for specific off-target binding interactions of a biotinylated BT7480 (BCY13582) at 1 μM. Detailed methods for the primary and confirmation screens can be found in the online supplemental materials.

Receptor occupancy assays

CD137 receptor occupancy was determined in isolated primary human PBMCs. Cryopreserved healthy human PBMCs were activated with anti-CD3 (BioLegend Cat. No. 317347) antibody overnight. Activated PBMCs were incubated with variable concentrations of TICA for 1 hour. PBMCs were then stained for viability (Zombie violet, BioLegend Cat. No. 423113) and subsequently stained with a master mix (anti-human CD4 (BD Biosciences Cat. No. 563875), anti-human CD8 (BioLegend Cat. No. 301045), BCY15416 (Alexa488-conjugated CD137 *Bicycle* dimer) and a non-competing total CD137 antibody (BioLegend Cat. No. 309808) at room temperature (RT) for 30 min. Cells were washed and resuspended in FACS (Fluorescence Activated Cell Sorting) buffer (1× PBS (Phosphate Buffered Saline) with 2% FBS (Fetal Bovine Serum)) and data was acquired on a BD Celesta flow cytometer. CD137 receptors unoccupied by TICA were labeled with BCY15416 and total CD137 levels were determined with the non-competing CD137 antibody. As the concentration of TICA increases, CD137 dimer binding decreases giving an inhibition curve. CD137 receptor occupancy was calculated using the following equation:

$$\% \text{ Receptor occupancy} = \left(1 - \frac{\text{Geometric Mean (Geo Mean)} - E_{\text{min}}}{E_{\text{max}} - E_{\text{min}}} \right) * 100$$

Nectin-4 receptor occupancy was determined in Nectin-4 expressing HT-1376 and T-47D cell lines in vitro. A549 (Nectin-4-negative) cells were used as a control. Cells were plated at a density of 1×10^5 cells/well and then treated with indicated concentrations of BT7480 or BCY13144 for 1 hour at 4°C. Cells were then stained with the viability dye (BioLegend Cat. No. 423113) at RT for 15 min. Cells were subsequently stained with a competing Nectin-4 antibody (R&D Systems Cat. No. FAB2659) or an isotype control (R&D Systems Cat. No. IC0041P) at RT for 30 min and then processed on the BD Celesta flow cytometer. Nectin-4 receptors unoccupied by BT7480 were labeled with the Nectin-4 antibody and percent Nectin-4 receptor occupancy was calculated as described above.

Pharmacokinetics of BT7480 in mouse and non-human primate

Male CD-1 mice were administered an intravenous bolus dose of BT7480 formulated in 25 mM histidine HCl, 10% sucrose pH7. Serial bleeding was performed at each time point. Male naïve cynomolgus monkeys were administered with a 15 min intravenous infusion of 1 mg/kg BT7480 on day 1 and 10 mg/kg on day 7. Serial bleeding was performed at each time point. Bioanalytical method has been described.¹⁴ Plasma concentration versus time data were analyzed by non-compartmental analysis (NCA) using the Phoenix WinNonlin V.6.3 software program. C_0 (for intravenous bolus), C_{max} , Cl , $V_{d_{ss}}$, $T_{1/2}$, $AUC_{(0-last)}$, $AUC_{(0-inf)}$, $MRT_{(0-inf)}$ and graphs of plasma concentration vs time profile were reported.

Syngeneic tumor models

Mouse efficacy and pharmacodynamic (PD) studies were performed in C57BL/6J-hCD137 mice (B-hTNFRSF9(CD137); Biocytogen, Beijing, China) with subcutaneously implanted MC38-Nectin-4 tumors or in BALB/c hCD137 mice (GemPharmatech, Nanjing, China) with subcutaneously implanted CT26-Nectin-4 tumors. Transcriptional profiling was performed for tumor RNA using nCounter mouse PanCancer IO 360 panel (NanoString) and for white blood cell (WBC) RNA using Mouse PanCancer Immune Profiling Panel and data were analyzed using the nSolver analysis software (NanoString) with advanced analysis probe set ns_mm_io_360_v1.0 or ns_mm_cancerImm_C3400. CD8+ tumor infiltrating cells were stained using anti-mouse CD8 antibody (Abcam, # ab217344) and Nectin-4 immunohistochemistry (IHC) was performed using an in-house developed anti-Nectin-4 antibody with Ventana Discovery OmniMap anti-Rb HRP Kit. See all details in online supplemental materials.

All the procedures related to animal handling, care and treatment in the studies were performed according to the guidelines approved by the Institutional Animal Care and Use Committee of WuXi AppTec (Beijing, China), following the guidance of the Association for Assessment and Accreditation of Laboratory Animal Care.

DRF study in rat (Wistar Han)

For the dose range finding (DRF) study in rat (Wistar Han, male, 6–7 weeks of age), 30, 100 or 300 mg/kg doses of BT7480 were administered by a 15 min intravenous infusion in vehicle (5% glucose in TRIS (tris(hydroxymethyl) aminomethane), pH 7–7.5) in a dose volume of 5 mL/kg. Four rats/group were assigned to the main study. Clinical observations included recording of clinical signs, individual body weight, food consumption, and ophthalmic assessments. Clinical pathology evaluations included samples for hematology (analyzed by ADVIA 2120i) and clinical chemistry (analyzed by AU680) on Day 8.

NHP cytokine quantification

To evaluate the ability of BT7480 to induce changes in circulating cytokines in healthy non-human primate (NHP), three naïve cynomolgus monkeys were each dosed with a 15 min intravenous infusion of BT7480 at 1 and 10 mg/kg a week apart as described above in the pharmacokinetic (PK) methods. Cytokine samples were collected at pre-dose (0 hour) on Day -7, 1 and 24 hours on Day 1, pre-dose (0 hour), 1 and 24 hours on Day 7, and pre-dose (0 hour) and on Day 14 post-dose. ProcartaPlex NHP Cytokine & Chemokine Panel 30-plex (Invitrogen) with Bio-Plex 200 instrumentation and software (Bio-Rad) was used to measure circulating cytokine levels from serum (EDTA as anti-coagulant) according to manufacturer's instructions.

DRF study in NHP (cynomolgus monkey)

BT7480 doses of 30, 100 or 300 mg/kg were administered by 15 min intravenous infusion in vehicle (5% glucose in TRIS, pH 7–7.5) in a dose volume of 5 mL/kg. At the initiation of dosing, monkeys were approximately 31–38 months of age. Two monkeys (one of each sex) were assigned to each group. Clinical observations included recording of clinical signs, mortality, body weight, and ECG parameters. Clinical pathology evaluations included samples for hematology and clinical chemistry on Days -7 and 8 (relative to dosing) analyzed with ADVIA 2120 (hematology) and AU680 (clinical chemistry, including liver function tests alanine aminotransferase, aspartate aminotransferase, alkaline phosphatase, glutamate dehydrogenase and total bilirubin).

RESULTS

Nectin-4-expressing and CD137-expressing cells are co-localized in human tumors

We set out to create a drug that activates CD137 only when co-ligated with Nectin-4 which necessitates that relevant immune cells come into direct contact with Nectin-4-expressing tumor cells. RNA expression analysis of 12,564 samples from 36 human cancer indications compiled by TCGA, indicated co-expression of Nectin-4 and CD137 across several tumor types including lung, breast, esophageal, stomach, ovarian, head and neck, pancreatic, and bladder (figure 1A).

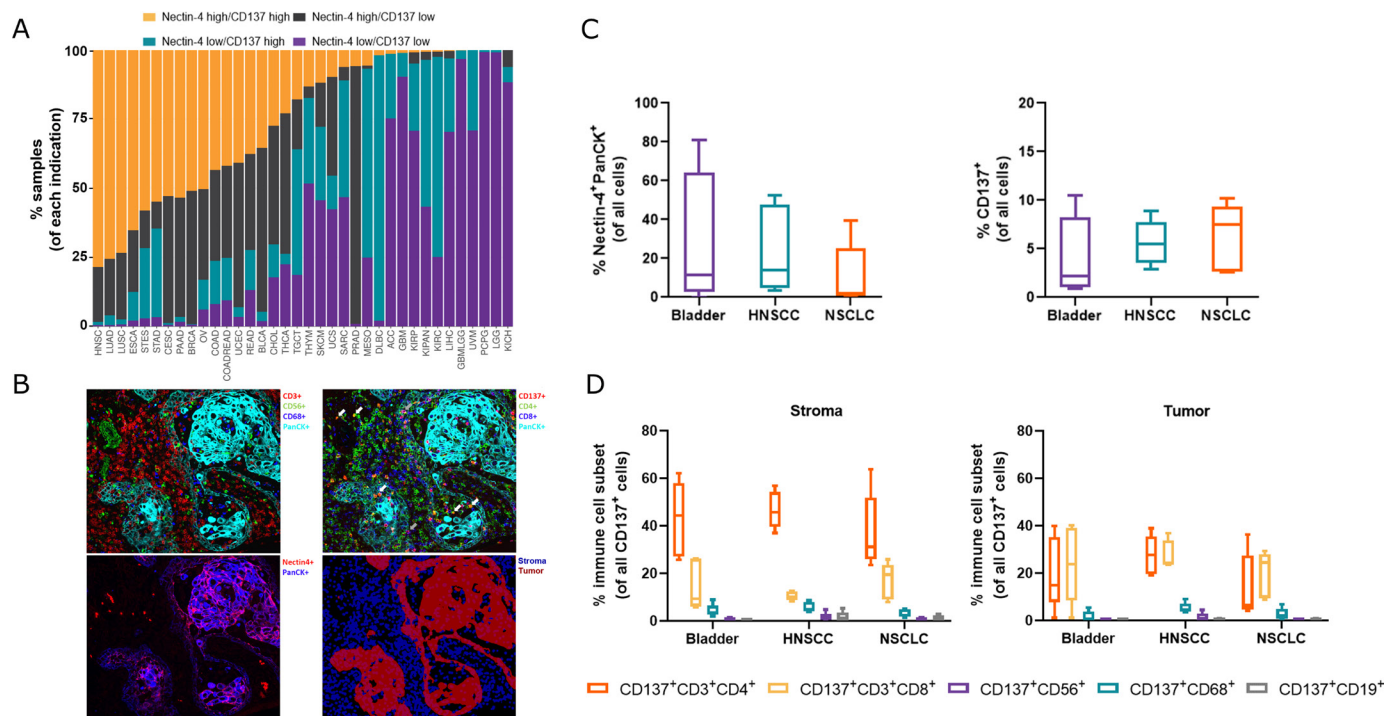


Figure 1 Nectin-4-expressing tumor cells and CD137-expressing immune cells co-localize in human cancers. (A) Transcript co-expression across tumor types in TCGA. (B) MultiOmyx imaging allows for simultaneous interrogation of immune infiltrate and spatial proteomic profiling within human tumors. A single ROI (Region Of Interest) from a representative HNSCC (Head and Neck Squamous Cell Carcinoma) sample is shown. T cells (CD3+, red), macrophages (CD68+, blue), NK cells (CD56+, green), and tumor cells (PanCK+, cyan) detected throughout tumor (top left). Examples of CD137+CD4+ and CD137+CD8+ T cells are shown and represented by white and gray arrows respectively (top right). Co-expression of Nectin-4 (red) and PanCK (blue) on tumor cells (bottom left). Tumor and stroma regions were identified using a PanCK and DAPI mask, respectively (bottom right, in red and blue, respectively). (C) Tumor Nectin-4 expression where total Nectin-4+PanCK+ cells are normalized to total cells (left) and CD137+ immune infiltrate where total CD137+ cells detected are normalized to total cells (right). Within each box, the horizontal line represents the mean of five samples shown. (D) Subset analysis of CD137+ immune infiltrate within stroma (left) and tumor (right) regions across samples and included T cells (CD3+CD4+ and CD3+CD8+), macrophages (CD68+), NK cells (CD56+), and B cells (CD19+). Data are total cells per phenotype normalized to total CD137+ cells detected across samples within each indication. Within each box, the horizontal line represents the mean of five samples shown. In (A): ACC, adrenocortical carcinoma; BLCA, bladder urothelial carcinoma; BRCA, breast invasive carcinoma; CESC, cervical squamous cell carcinoma and endocervical adenocarcinoma; CHOL, cholangiocarcinoma; COAD, colon adenocarcinoma; COADREAD, colorectal adenocarcinoma; DLBC, diffuse large B-cell lymphoma; ESCA, esophageal carcinoma; GBM, glioblastoma multiforme; GBMLGG, glioma; HNSC, head and neck squamous cell carcinoma; KICH, kidney chromophobe; KIPAN, Pan-kidney cohort (KICH+KIRC+KIRP); KIRC, renal clear cell carcinoma; KIRP, renal papillary cell carcinoma; LGG, brain lower grade glioma; LIHC, hepatocellular carcinoma; LUAD, lung adenocarcinoma; LUSC, lung squamous cell carcinoma; MESO, mesothelioma; NK, natural killer; OV, ovarian serous cystadenocarcinoma; PAAD, pancreatic adenocarcinoma; PCPG, pheochromocytoma and paraganglioma; PRAD, prostate adenocarcinoma; READ, rectum adenocarcinoma; SARC, sarcoma; SKCM, skin cutaneous melanoma; STAD, stomach adenocarcinoma; STES, esophagus-stomach cancers; TCGA, The Cancer Genome Atlas; TGCT, testicular germ cell tumors; THCA, thyroid carcinoma; THYM, thymoma; UCEC, uterine corpus endometrial carcinoma; UCS, uterine carcinosarcoma; UVM, uveal melanoma.

More than half of the tumor types examined had a substantive proportion of tumors that expressed high levels of both Nectin-4 and CD137 (figure 1A). Based on these data, we selected three major tumor types, namely NSCLC, HNSCC and bladder cancers to further examine Nectin-4 and CD137 in human tumors via spatial proteomic profiling. A MultiOmyx assay was developed and used to quantify simultaneously the presence of Nectin-4-positive and CD137-positive cells and their spatial topography in 15 human tumor samples (figure 1B–D). We found abundant but variable staining (expression) of Nectin-4 and CD137,

confirming expectations based on the TCGA data. Spatial profiling analysis discriminating tumor core versus tumor stroma revealed CD137-positive immune infiltrates within the tumor cores where Nectin-4-positive tumor cells are located (figure 1D). CD137-expressing immune cells were largely comprised of CD4-positive and CD8-positive T cells, but also a consistent fraction were myeloid lineage cells based on co-staining for CD68 (figure 1D). These data indicate that the action of a CD137 TICA might not be limited to T cells and that both cell types are likely to contact tumor cells bearing Nectin-4.

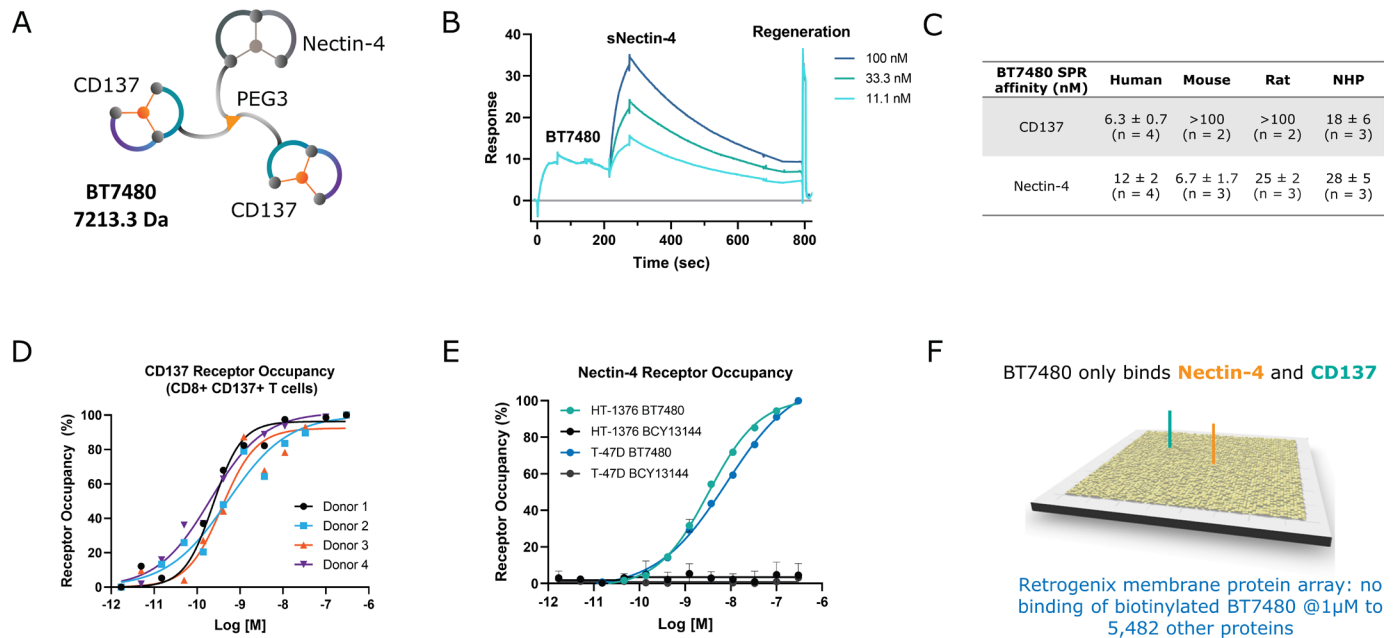


Figure 2 BT7480 binds potently and specifically to both tumor and immune cell targets. (A) Schematic of the BT7480 structure, which is comprised of three bicyclic peptides, one that binds to Nectin-4 and two (that are identical to each other) that bind to CD137 and are conjugated together via a three-arm branched PEG3 linker. (B) Sensorgram for representative SPR binding experiment where BT7480 is first captured to sensor surface immobilized human CD137 followed by binding of soluble human Nectin-4 at different concentrations. (C) Affinity of BT7480 for sNectin-4 and sCD137 across four species (human, mouse, rat, and NHP) while simultaneously bound to immobilized human CD137 or Nectin-4 as determined by SPR. (D) Human peripheral blood mononuclear cells (Donors 1-4) were stimulated with anti-CD3 overnight and subsequently treated with BT7480 for 1 hour. Unbound CD137 receptors following BT7480 treatment and total CD137 receptors were detected by flow cytometry using an AlexaFluor 488-labeled CD137 *Bicycle* dimer (BCY15416) and a non-competitive CD137 antibody, respectively. Receptor occupancy was calculated as described in the Methods. (E) HT-1376 and T-47D cells were treated with either BT7480 or a non-Nectin-4 binding analog of BT7480 (BCY13144) for 1 hour. BT7480 Nectin-4 receptor occupancy was determined by flow cytometry using a competitive Nectin-4 antibody. Data are mean/SD. (n=3 replicates). Data in (D) and (E) were fit using log(agonist) versus response—variable slope (four parameter) in GraphPad Prism V.8.4.3. (F) Cartoon representation summarizing the results of a cell microarray screen (Retrogenix) designed to look for specific off-target binding interactions of a biotin-tagged analog of BT7480 (BCY13582). The screen tested for binding against human HEK293 cells individually expressing 5484 full-length human plasma membrane proteins and tethered secreted proteins. BCY13582 only bound specifically to Nectin-4 and CD137. NHP, non-human primate; SPR, surface plasmon resonance.

BT7480 binds potently and specifically to its human targets

BT7480 is comprised of three *Bicycles*, one that binds to Nectin-4 and two that bind to CD137, conjugated together via a three-arm branched-polyethylene glycol (PEG3) linker (figure 2A). The CD137 binding *Bicycle* shares an epitope with the natural ligand of CD137, CD137L¹⁴ and online supplemental figure S1). The medicinal chemistry and structure activity relationship investigation for selecting BT7480 as a development candidate will be described elsewhere (Upadhyaya *et al* in preparation). The affinity of BT7480 for mouse, rat, NHP, and human CD137 and Nectin-4 was determined using a surface plasmon resonance assay where BT7480 is simultaneously bound to both receptors. To measure the affinity for CD137, BT7480 was bound to immobilized human Nectin-4 and soluble CD137 (sCD137) served as the analyte. Similarly, to measure the affinity for Nectin-4, BT7480 was bound first to immobilized human CD137 and soluble Nectin-4 served as the analyte (figure 2B). BT7480 bound with high affinity to human ($K_D=6$ nM) and cynomolgus monkey ($K_D=18$ nM) sCD137 and did

not bind to mouse or rat sCD137 (figure 2C and online supplemental figure S2). BT7480 bound with high affinity to human ($K_D=12$ nM), cynomolgus monkey ($K_D=28$ nM), mouse ($K_D=7$ nM), and rat ($K_D=25$ nM) sNectin-4 (figure 2C and online supplemental figure S3). Binding of BT7480 was specific to Nectin-4 and CD137 and it did not bind to other known family members (online supplemental table 1). We next explored the ability of BT7480 to bind to its targets on cells. A novel CD137 receptor occupancy assay using a labeled CD137 *Bicycle* dimer (BCY15416, Alexa Fluor 488) as a probe to detect CD137 not occupied by BT7480 was developed (online supplemental figure S4A–D). A non-competing CD137 antibody was used to monitor total CD137 cell surface expression levels. Dose-dependent CD137 receptor occupancy was observed for BT7480 in the CD8 +CD137+ population of anti-CD3 stimulated human PBMCs across four donors (figure 2D). BCY12797, an enantiomeric non-CD137 binding analog of BT7480 did not occupy CD137 receptors demonstrating specificity with respect to CD137 (online supplemental figure S4E). An AF488-labeled derivative of

BT7480 (BCY13583) was used in a direct binding assay to further demonstrate specific binding to CD137 + T cells in stimulated human PBMCs (online supplemental figure S5A–D). To measure the ability of BT7480 to bind to Nectin-4 expressed on human tumor cell lines, a receptor occupancy assay was developed using a commercially available antibody that competed with BT7480 for binding to Nectin-4. BT7480 occupied Nectin-4 expressed on HT-1376 and T-47D cells in a dose dependent manner, whereas an enantiomeric non-Nectin-4 binding analog of BT7480 (BCY13144) did not compete with the antibody (figure 2E). Furthermore, BT7480 did not bind to the Nectin-4-negative A549 cells (online supplemental figure S6). A cell microarray technology (Retrogenix) was used to assess the selectivity of BT7480 to 5484 human plasma membrane proteins and cell surface tethered secreted proteins. Biotinylated-BT7480 bound only to Nectin-4 and CD137 indicating that the *Bicycles* are highly specific binding moieties (figure 2F).

BT7480 elicits potent Nectin-4-dependent CD137 agonist activity in vitro

The functional activity of BT7480 was evaluated using a CD137 reporter assay with tumor cell lines as sources of tumor antigen. BT7480 demonstrated sub-nanomolar potency for CD137 agonism in this model system with co-cultured Jurkat-CD137 reporter cells and 4T1 mouse tumor cells engineered to overexpress Nectin-4 (figure 3A, right panel). There was no induction of reporter activity when the Jurkat-CD137 reporter cells were co-cultured with target null 4T1 parental cells (figure 3A, left panel) and a non-CD137 binding control (BCY12797) did not induce CD137 agonism. In contrast and as expected, the anti-CD137 antibody agonist induced CD137 agonism in a Nectin-4-independent manner. BT7480 also induced CD137 agonism when reporter cells were co-cultured with the Nectin-4-expressing human cancer cell line, HT-1376 (figure 3B). The activity of an anti-CD137 antibody agonist and CD137L in this assay system are shown for comparison. To evaluate the activity of BT7480 in a human primary cell system, PBMCs were co-cultured with the Nectin-4-expressing mouse 4T1 cells described earlier and then treated with anti-CD3 to stimulate CD137 expression on immune cells. Levels of interferon gamma (IFN γ) and interleukin (IL)-2 in the culture supernatant increased with treatment of BT7480 in a dose-dependent manner (figure 3C, right panels). The activity of BT7480 was dependent on the presence of the Nectin-4-expressing cells as there was minimal induction of cytokine secretion in co-culture with 4T1 parental cells (figure 3C, left panels, online supplemental figure S7). BT7480 activity was also dependent on its ability to bind to CD137 since BCY12797 was inactive. Increased IFN γ and IL-2 secretion in response to BT7480 treatment was also observed when human PBMCs were co-cultured with Nectin-4-expressing HT-1376 cells and the activity was superior to an anti-CD137 antibody agonist in this assay system (figure 3D, online supplemental figure S8). Of

note, in both the reporter and primary co-culture assay system, BT7480 exhibited lower activity at higher doses when one or both targets became limiting, a bioactivity profile that is referred to as a ‘hook effect’ and is expected for bispecific molecules that form ternary complexes.²⁵ In addition to HT-1376 cells, the activity of BT7480 was both potent and Nectin-4-dependent in the co-culture model with mouse or other human Nectin-4-expressing cancer cell lines (online supplemental figure S9A–C). Furthermore, BCY13144, the non-Nectin-4 binding analog of BT7480 was inactive (online supplemental figure S10). Unsurprisingly, BT7480 did not trigger cytokine release in human whole blood (online supplemental figure S11).

BT7480 drives CD8+ T cell tumor infiltration, tumor regressions and complete responses in vivo

BT7480 has a terminal plasma half-life of approximately 2.3 hours in mice (figure 4A) which allowed us to investigate the efficacy of intermittent BT7480 plasma exposure in syngeneic mouse tumor models. Mice bearing subcutaneous MC38-Nectin-4 tumors were treated intravenously with BT7480 at 3 and 10 mg/kg per week with two dosing schedules (once a week (QW) or dose fractionated twice a week (BIW)). BT7480 was efficacious, reducing tumor growth and causing complete regressions (CRs) with the rate of CRs ranging from 0/6 (3 mg/kg QW) to 6/6 (5 mg/kg BIW) by day 21 (figure 4C). The plasma target coverage profiles for BT7480 dosing regimens in mice (figure 4B,D) were simulated based on mouse plasma concentrations and the average EC50 for BT7480 mediated induction of IFN γ and IL-2 secretion (online supplemental figure S9). The 5 mg/kg BIW dosing regimen that led to maximal efficacy has a plasma PK profile that maintained target coverage for approximately 1 day to 2 or 3 days apart in a weekly dosing cycle. Next, we tested a dosing regimen (5 mg/kg at 0 and 24 hours) which would lead to nearly continuous target coverage over the first 2 days of the weekly dosing cycle. The same total weekly dose (10 mg/kg) was given at 0 hour as a comparator since the time of target coverage is vastly different (figure 4D) even though the total dose remains identical. While both dosing regimens had significant antitumor activity, 5 mg/kg dosing at 0 and 24 hours was superior with 4/6 CRs to the 10 mg/kg dosing with 1/6 CRs by day 15. Furthermore, a dosing regimen of 5 mg/kg at 0, 24, and 48 hours did not yield additional antitumor activity (1/6 CRs) (figure 4E). Thus, the maximum antitumor activity of BT7480 could be reached by continuous plasma target coverage of approximately 2 days within a weekly dosing cycle.

Mice that achieved CR after treatment with BT7480 proved resistant to rechallenge with MC38-Nectin-4 tumor cell implantation. In contrast, CR mice depleted of CD8 + T cells allowed for development of 8 tumors out of 10 implanted mice indicating that this resistance was dependent on CD8 + T cells (figure 4F, online supplemental figure S13).

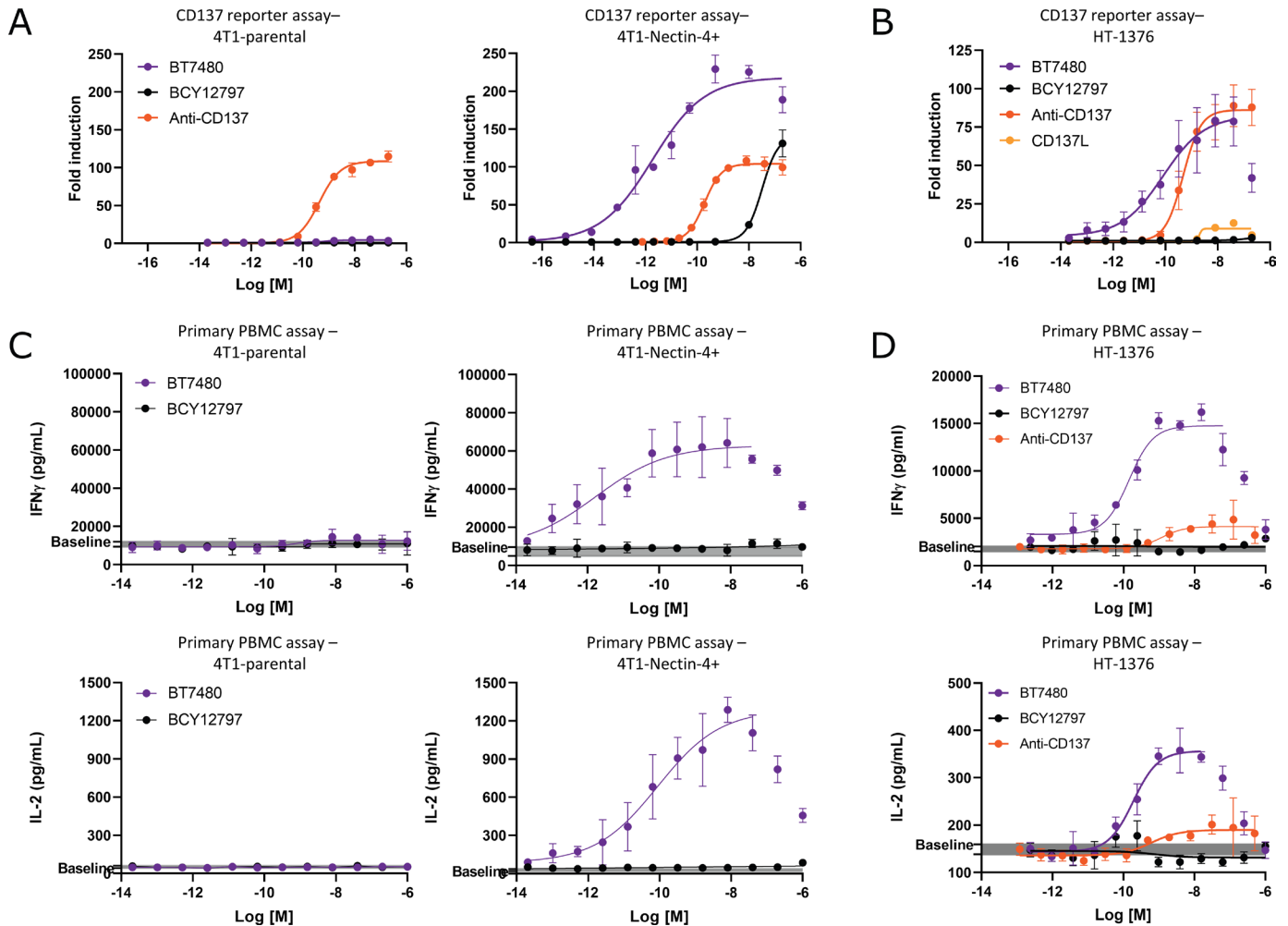


Figure 3 BT7480 elicits potent Nectin-4-dependent CD137 agonist activity in vitro. (A) Jurkat cells expressing human CD137 coupled to a NFκB (Nuclear Factor kappa-light-chain-enhancer of activated B cells)-driven luciferase reporter gene were co-cultured with mouse 4T1 cells or mouse 4T1 cells that were engineered to overexpress mouse Nectin-4 (4T1-Nectin-4) and treated for 6 hours with BT7480, an enantiomeric non-CD137 binding analog of BT7480 (BCY12797), or an anti-CD137 antibody agonist. Activity was read out as reporter gene product activity and BT7480 activity was dependent on Nectin-4 expression and on the ability of the molecule to bind CD137. Data are mean/SD (n=3 replicates). (B) Jurkat-CD137 reporter cells were co-cultured with Nectin-4-expressing HT-1376 cells and treated with BT7480, BCY12797, anti-CD137 antibody agonist, or the natural ligand of CD137 (CD137L). Data are mean/SD (n=3 replicates). (C) Human PBMCs (donor 231356) were stimulated with anti-CD3 and co-cultured with mouse 4T1 or 4T1-Nectin-4 cells and treated with BT7480 or BCY12797 and IFN γ and IL-2 in the culture supernatants was measured after 48 hours. The gray bar indicates untreated control levels. Data are mean/SD (n=3 replicates). (D) Human PBMCs (donor 228769) were stimulated with anti-CD3 and co-cultured with human HT-1376 cells and treated with BT7480, BCY12797, or anti-CD137 antibody agonist and IFN γ and IL-2 in the culture supernatants were measured after 48 hours. The gray bar indicates untreated control levels. Data are mean/SD (n=3 replicates). Data in all plots were fit using log(agonist) versus response (three parameter) or log(agonist) versus response—variable slope (four parameter) in GraphPad Prism V.8.4.3. IFN, interferon; IL, interleukin; PBMC, peripheral blood mononuclear cell.

To gain further insights into the activity of BT7480, a CT26-Nectin-4 syngeneic tumor model was also evaluated. This model has slower response kinetics to BT7480 and thus permitted analysis of the tumor by flow cytometry. Mice bearing subcutaneous CT26-Nectin-4 tumors were treated with BT7480 at two doses (1 and 5 mg/kg) with two dosing schedules (once a day (QD) at 1 mg/kg or every 3 days (Q3D) at 1 and 5 mg/kg). BT7480 was efficacious, reducing tumor growth significantly in response to 5 mg/kg Q3D dosing (figure 4G). The tumor tissue was analyzed on day 15 and a significant

increase of total T cells (CD3 +CD45+) and CD8 + T cells (CD8 +CD3+CD45+) was observed in tumor tissue after 1 mg/kg QD and 5 mg/kg Q3D BT7480 treatment (figure 4H). Blood samples from the mice on day 15 were analyzed for liver enzymes (alanine aminotransferase, aspartate aminotransferase and alkaline phosphatase). No significant changes in any of these markers of hepatic function were detected in response to BT7480 treatment (online supplemental figure S14). BT7480 activity in the CT26 -based tumor model was shown to be limited to

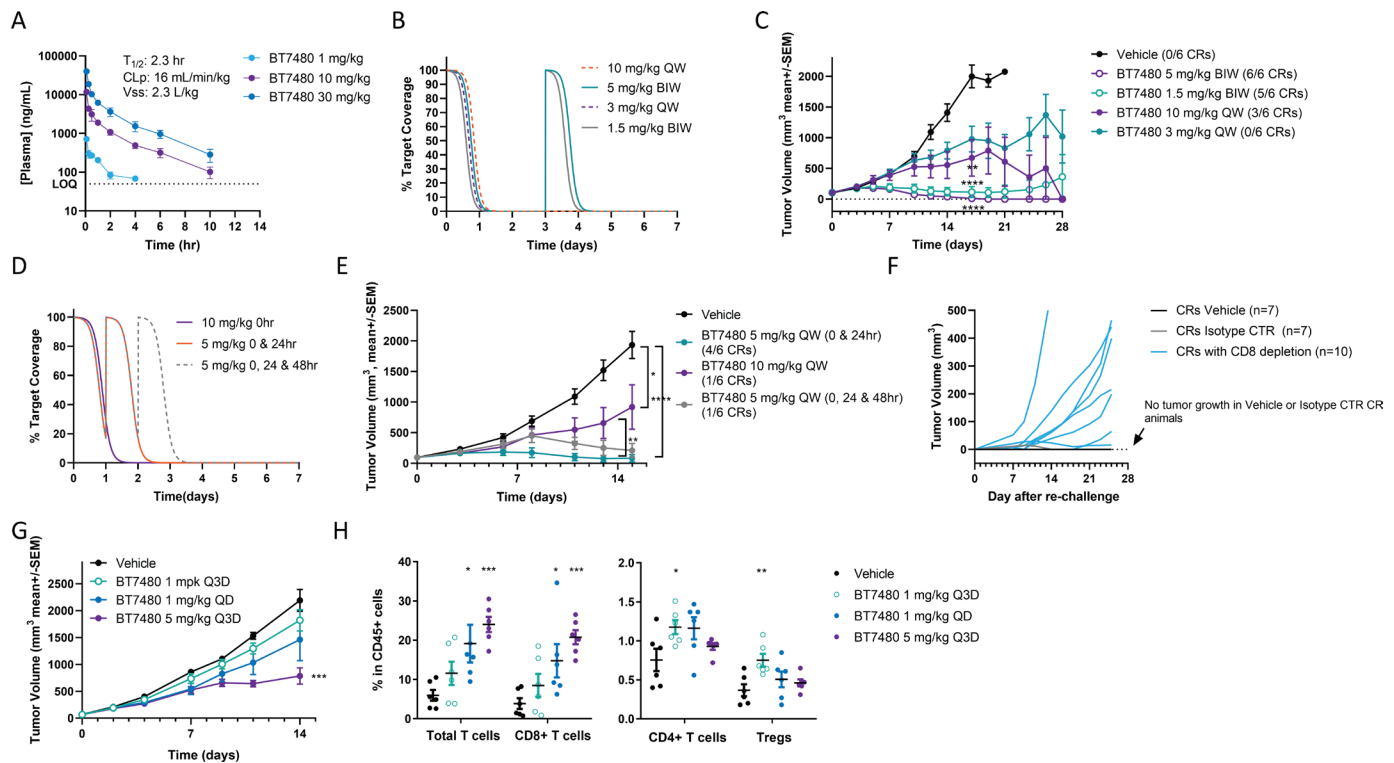


Figure 4 BT7480 leads to tumor regressions and complete responses in vivo without continuous drug exposure in the periphery. (A) BT7480 concentration and PK parameters in plasma after a 1, 10 and 30 mg/kg intravenous bolus dose in CD-1 mice. (B) Simulated target coverage–time profile of BT7480 dosed twice a week (BIW) with 1.5 mg/kg and 5 mg/kg or weekly (QW) with 3 and 10 mg/kg. (C) MC38-Nectin-4 tumor growth in huCD137 C57Bl/6 mice with weekly or twice a week dosing of BT7480 ($n=6/\text{cohort}$; $**<0.01$, $****p<0.0001$ two-way analysis of variance (ANOVA), with Dunnett's post-test, days 0–17). Number of complete responders (CRs) are indicated in the figure. (D) Simulated target coverage–time profile of BT7480 dosed at 10 mg/kg at 0 hour, 5 mg/kg at 0 and 24 hours and 5 mg/kg at 0, 24 and 48 hours. (E) MC38-Nectin-4 tumor growth in huCD137 C57Bl/6 mice with weekly total dose of 10 mg/kg BT7480 administered either as one 10 mg/kg dose at 0 hour or fractionated to two doses of 5 mg/kg at 0 and 24 hours of a weekly dosing cycle. 5 mg/kg at 0 and 24 hours was also compared to 5 mg/kg at 0, 24 and 48 hours weekly dosing regimen ($n=6/\text{cohort}$; $*p<0.05$, $**<0.01$, $****p<0.0001$ mixed-effects analysis days 0–15). Number of CRs are indicated in the figure. (F) CR mice from the study shown in C were rechallenged on day 59 after treatment initiation with or without CD8+ T cell depletion (or treatment with isotype control antibody). Note that no tumor growth was observed in vehicle or isotype control treated CR mice whereas 8/10 CR mice with CD8+ T cell depletion showed tumor growth. (G) CT26-Nectin-4 tumor growth in huCD137 Balb/c mice with intermittent (5 mg/kg every 3 days (Q3D)) or daily (1 mg/kg once a day (QD)) intraperitoneal dosing of BT7480 ($n=6/\text{cohort}$; $***p<0.001$, two-way ANOVA, with Dunnett's post-test). (H) End of study tumors from (G) were analyzed for T cell infiltration on day 15 after treatment initiation ($*p<0.05$, $**p<0.01$, $***p<0.001$, one-way ANOVA with Dunnett's post-test). CLp, plasma clearance; LOQ, limit of quantitation; $T_{1/2}$, terminal plasma half-life; Vss, volume of distribution at steady state. Individual tumor growth curves (C, E and G) are shown in online supplemental figure S12.

Nectin-4 expressing CT26 tumors (online supplemental figure S15).

BT7480 causes rapid activation of tumor immune signaling followed by T cell infiltration

To evaluate the PD effects of BT7480 in the tumor immune microenvironment, IHC and NanoString messenger RNA (mRNA) profiling of MC38-Nectin-4 tumors was conducted. Tumors were harvested 24, 48, 96 and 144 hours after BT7480 treatment (5 mg/kg, 0 and 24 hours) or 144 hours after treatment with a non-CD137 binding control (NB-BCY/BCY12797, 5 mg/kg, 0 and 24 hours) or an anti-CD137 antibody agonist (2 mg/kg). IHC evaluation of Nectin-4 expression in tumors revealed that expression was low and heterogeneous. Overall, a minority of tumor cells stained positive for Nectin-4 and

the variation of the Nectin-4 positivity across different areas of the same tumor was large (figure 5A). Despite this low and heterogeneous expression profile for Nectin-4, IHC analysis of tumors treated with BT7480 at 144 hours revealed striking and pervasive T cell infiltrates that were absent in tumors of vehicle or NB-BCY treated animals and increased in tumors of anti-CD137 antibody agonist-treated animals (figure 5B). mRNA profiling revealed a profound reprogramming of the tumor immune microenvironment at 144 hours by BT7480 and to lesser extent by the anti-CD137 antibody agonist (figure 5C). Several immune checkpoint mRNAs were significantly upregulated by BT7480, consistent with immune pressure on the tumor and activation of a T cell response. BT7480 also upregulated Cxcl9, a chemokine whose expression is a

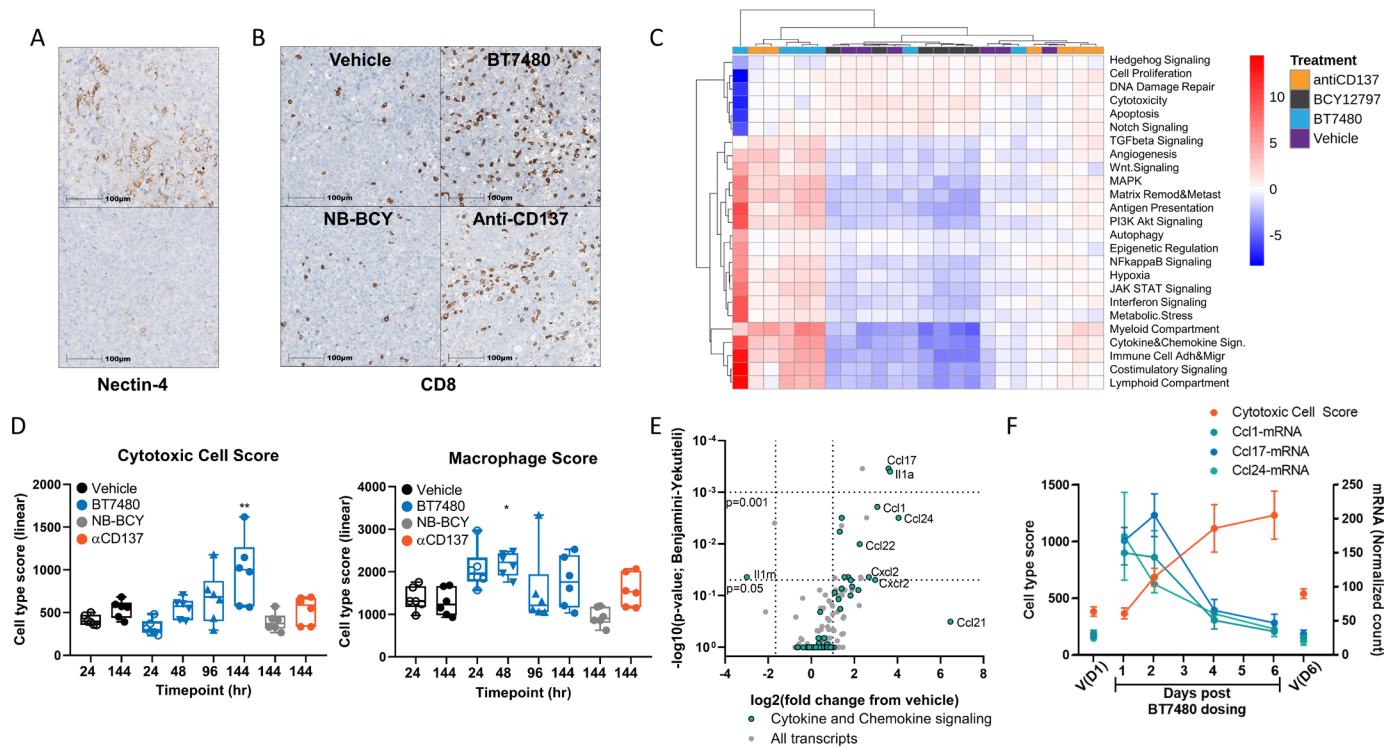


Figure 5 BT7480 causes rapid activation of tumor immune signaling followed by T cell infiltration. (A) Nectin-4 staining of two areas from the same vehicle treated MC38-Nectin-4 tumor is shown demonstrating the range of Nectin-4 expressing MC38 tumor cells within the tissue. (B) Representative images of tissue sections harvested at 144-hour time point from tumors treated with vehicle, 5 mg/kg BT7480 or NB-BCY (BCY12797) at 0 and 24 hours or 2 mg/kg anti-CD137 antibody agonist every 3 days and stained for mouse CD8 are shown. (C) NanoString analysis of tumors at 144-hour time point show the immunomodulatory effect of BT7480 and anti-CD137 antibody agonist on the 25 functional pathways including stimulation of NFκB signaling, costimulatory signaling, cytokine/chemokine signaling and interferon signaling among others. Red indicates high signature scores; blue indicates low scores. Scores are displayed on the same scale via a Z-transformation. (D) NanoString analysis of tumors show the effect of BT7480 from 24 to 144 hours and anti-CD137 antibody agonist at 144 hours on the cytotoxic cell (probe set: Ctsw, Gzma, Gzmb, Klr1, Klrd1, Klrk1, Nkg7 and Prf1) and macrophage (probe set: CD163, CD68, CD84 and Ms4a4a) content. * $p < 0.05$, ** $p < 0.01$, one-way analysis of variance with Dunnett's post-test, (24 hours vehicle used for 24, 48 and 96 hour time points, 144 hours vehicle used for the 144-hour time point). (E) Transcriptional changes induced by BT7480 at 24-hour time point. Gray circles represent all measured transcripts and aqua circles identify transcripts belonging to the gene set for 'Cytokine and chemokine signaling'. Note that y-axis denotes adjusted (Benjamini-Yekutieli) p values. (F) Cytotoxic cell scores (left y-axis) and Ccl1-, Ccl17- and Ccl24- mRNA counts (right y-axis) overlaid over the course of the study (days post dosing). mRNA, messenger RNA.

strong predictor of checkpoint inhibitor response across many tumor types²⁶ (online supplemental figure S16). Analysis of the entire data set revealed that treatment of BT7480 resulted in an early increase (significant by 48 hours) of the macrophage score followed by an increase in the cytotoxic cell score by 144 hours (figure 5D). This indicates that a wider reprogramming of the immune microenvironment beyond T cells may occur early after BT7480 administration. Indeed, analysis of the earliest time points revealed that the majority of the top 20 differentially expressed genes belonged to cytokine and chemokine, co-stimulatory, and NFκB signaling pathway gene sets implying an early BT7480-induced cytokine transcription from cell types beyond T cells (figure 5E and online supplemental table S3). mRNA in situ hybridization studies on Ccl17- and Ccl22-mRNAs excluded Cd3-mRNA positive cells as the source of the cytokine expression (online supplemental figure S17), but the

identity of these cells is still unknown. Overlaying the time course of mRNA levels for Ccl17, Ccl1 and Ccl24 with the cytotoxic cell score (figure 5F), illustrates the kinetics of the immunomodulatory events after BT7480 administration: early increase of T cell chemotactic cytokine transcription followed by an increase in cytotoxic cell scores.

BT7480 causes monitorable changes in the transcriptional profiles of circulating WBCs

MC38-Nectin-4 tumor bearing C57BL/6J-hCD137 mice were treated intravenously with vehicle, BT7480, or NB-BCY at 5 mg/kg and an anti-CD137 antibody agonist at 0.2 mg/kg. NanoString transcriptional analysis was performed on WBCs harvested 24 hours after treatment. While no functional pathways were significantly enriched in treatment groups, 14 unique transcripts were significantly ($p < 0.05$, Benjamini-Yekutieli) modulated in response to BT7480 treatment and two in response

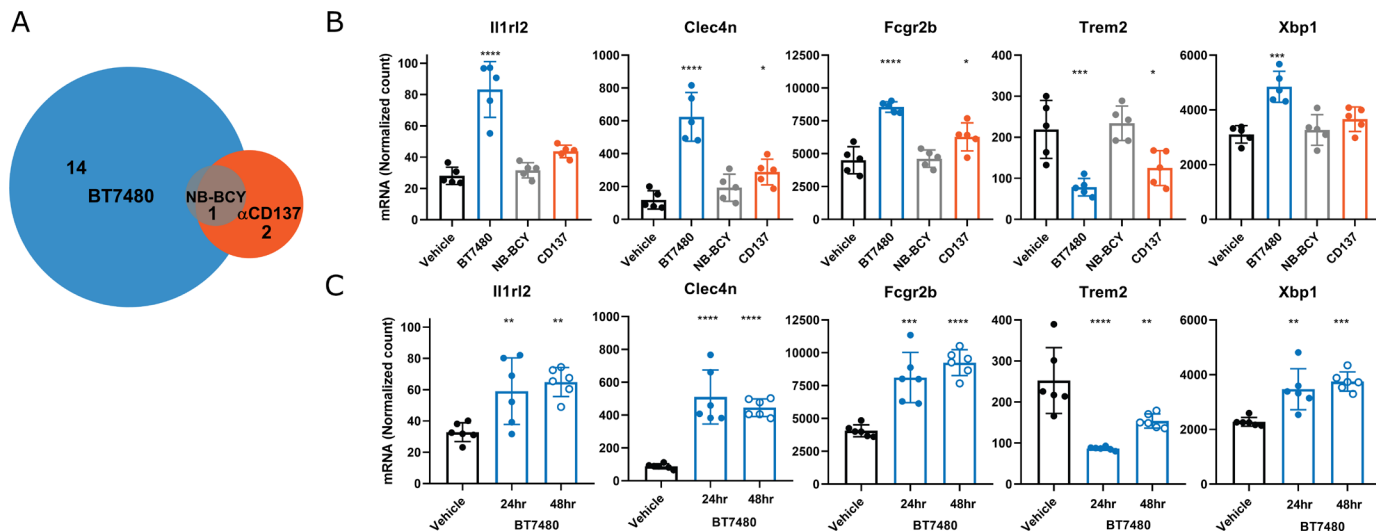


Figure 6 Transcriptional changes after BT7480 dosing are detectable in circulating white blood cells (WBCs). (A) Differentially expressed genes in circulating WBCs were identified from NanoString Mouse PanCancer Immune Profiling assay. VENN diagram showing the number of unique and shared transcripts (see online supplemental table S4 for full details) which are differentially expressed in WBCs from MC38-Nectin-4 bearing mice treated with 5 mg/kg BT7480 or non-CD137 binding control (NB-BCY/BCY12797) or 0.2 mg/kg anti-CD137 antibody agonist 24 hours after dosing. Differentially expressed genes were identified with NanoString Mouse PanCancer Immune Profiling assay. (B) mRNA levels of the top five differentially expressed transcripts in samples from BT7480 treated mice in study in panel A. (C) mRNA levels of the same top five transcripts in WBCs of mice 24 and 48 hours after treatment with vehicle or 5 mg/kg BT7480 at 0 and 24 hours from the study described in figure 6figure 5. * $p < 0.05$, ** $p < 0.01$, *** $p < 0.001$, **** $p < 0.0001$, one-way analysis of variance with Dunnett's post-test (24-hour vehicle used for both 24 and 48 hour analysis in panel C). mRNA, messenger RNA.

to anti-CD137 antibody agonist treatment (figure 6A and online supplemental table 4). WBCs harvested at 24 and 48 hours after BT7480 dosing from the tumor profiling study described above (shown in figure 5) were analyzed to confirm these findings. We took the top five differentially modulated transcripts from the initial WBC profiling study (figure 6B) and demonstrated that they were significantly modulated by BT7480 at the early time points (figure 6C). This supports the use of WBC transcriptional profiling to monitor immunomodulatory activity of BT7480 treatment in vivo.

BT7480 dosing is well tolerated in rats and NHPs

As part of the preclinical development program for BT7480, rodent and primate studies were performed. A PK-PD study in NHPs was conducted using doses of 1 mg/kg and 10 mg/kg BT7480 administered 1 week apart. All animals tolerated the BT7480 dosing well with no observed adverse effects. BT7480 showed dose linear PKs with similar clearances at 1 and 10 mg/kg and mean circulating plasma half-life of 6.7 hours (figure 7A). Measured cytokine levels were low throughout the study (most were below the limit of quantitation, (online supplemental table 5) and no significant increases in cytokines were observed after BT7480 treatment. A transient decrease of IL-8 was detected 1 hour after BT7480 treatment (figure 7B). Overall, the findings in healthy NHPs were unremarkable after 1 mg/kg and 10 mg/kg BT7480 dosing.

To define a BT7480 dose range suitable for the GLP BT7480 safety studies, a DRF study was performed in both

rat (Wistar Han) and NHP (Cynomolgus monkey). Rat was chosen as an animal model as it is an accepted rodent species for non-clinical toxicity testing by regulatory agencies. The cynomolgus monkey was chosen as the relevant non-rodent species due to binding of BT7480 to cynomolgus monkey Nectin-4 and CD137 (figure 2C).

BT7480 was administered to both species as a single administration by 15 min intravenous infusion at doses of 30, 100 and 300 mg/kg. No mortality was observed during the in-life phase or following administration in rat and there were no noteworthy treatment-related findings regarding ophthalmic examination, body weight, food consumption, hematology, or clinical chemistry parameters (figure 7C). In cynomolgus monkeys, there were no clinical observations considered to be BT7480-related following administration and there were no noteworthy treatment-related findings regarding ECG parameters, body weight, food consumption, or clinical chemistry or hematology parameters (figure 7C, online supplemental figure S18). Importantly, unlike what has been reported with other TNF receptor agonists,^{7,27} there were no signs of impact on the liver following BT7480 treatment.

DISCUSSION/CONCLUSION

Immunomodulation via agonism of TNF receptor superfamily members, in particular CD137, is a promising and resurgent anticancer therapeutic strategy.^{9-11 28-32} We recently reported the feasibility and proved the general concept for constructing tumor targeted TNF receptor

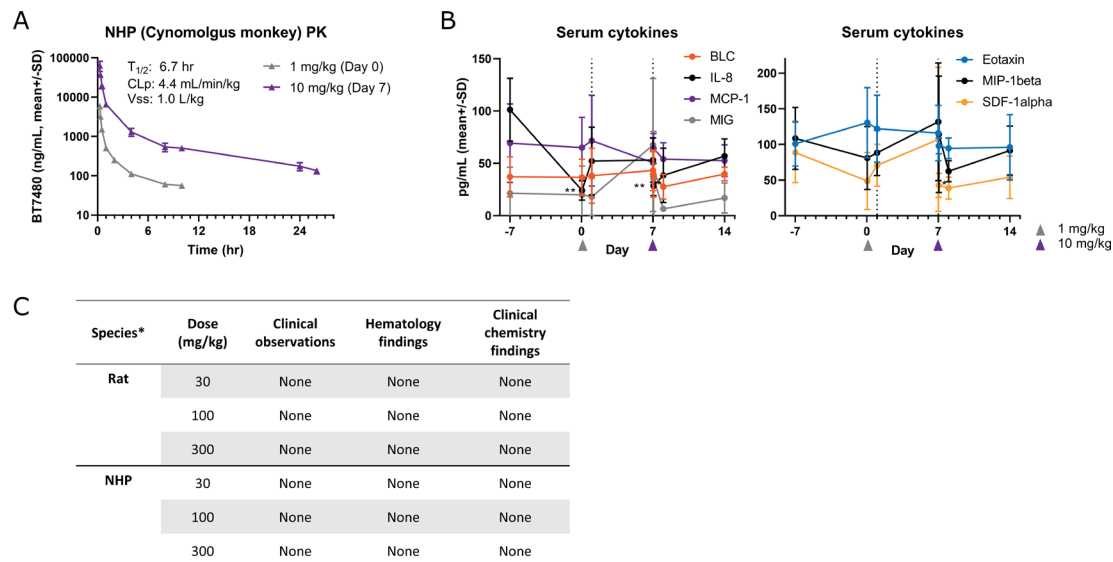


Figure 7 BT7480 dosing in rat and NHP is well tolerated with no adverse findings. (A) BT7480 plasma concentrations and mean PK parameters after an intravenous infusion of 1 mg/kg (on day 0) or 10 mg/kg (on day 7) over 15 min. PK parameters in the figure inset are mean values after both doses (n=3 animals/dose). (B) Levels of circulating cytokines were monitored throughout a 3-week period before and after BT7480 administration at 1 mg/kg or 10 mg/kg 15 min intravenous infusion in NHP. Of the detectable (above lower limit of quantitation in majority of samples) cytokines, BT7480 induced significant (**p<0.01, Student's t-test versus day -7 baseline) changes (transient decrease) only in IL-8 levels. (C) BT7480 doses (single dose) up to 300 mg/kg (15 min intravenous infusion) were well tolerated in a dose range finding study in rat and NHP with no clinical observations or noteworthy treatment related findings in clinical chemistry and hematology panels. *Rat = Wistar Han; NHP = Cynomolgus monkey. IL, interleukin; NHP, non-human primate; PK, pharmacokinetic .

agonists from fully synthetic component *Bicycle* monomers¹⁴ and characterized an EphA2-targeted CD137 agonist, BCY12491, which enhanced immune cell activation in co-culture with antigen-bearing tumor cell lines in vitro and caused complete rejection of tumors in vivo. In this work, we have reduced the concept to practice and developed a Nectin-4-targeted CD137 agonist, BT7480, that has both the desired bioactivity profile and the pharmaceutical properties that make it fit for regulatory consideration with a view to testing in patients with cancer. BT7480 activates CD137 signaling and function in vitro in a way that is dependent on co-ligation with Nectin-4 and in vivo causes elimination of tumors with development of immunological memory. This was accomplished without a need for continuous systemic exposure and without signs of hepatotoxicity in preclinical species.

The design goals for BT7480 included having no functional agonist activity on CD137 in the absence of Nectin-4 in order to limit activity to the tumor. Since BT7480 has high affinity for Nectin-4 and CD137 both separately and at the same time (figure 2), it can engage immune cells first, which then encounter Nectin-4 on tumor cells, or it can engage Nectin-4 in the tumor first and then be detected by CD137 on passing or adjacent resident immune cells. Either way, the mechanism of action necessitates juxtaposition, at least transiently, of CD137-positive immune cells and Nectin-4-positive tumor cells with implications for which patients/tumor types stand to benefit from BT7480 therapy. By profiling both transcript and protein expression we found good evidence for

CD137-positive immune cells being in the proximity of Nectin-4-positive tumor cells in a substantive proportion of patients across several tumor types with high unmet medical need (figure 1).

Equally important in developing an understanding of what patients might benefit the most was for us to gain a deeper insight into the mechanism of action of BT7480 as well as flexibility in the dosing regimen. We first learned from the series of mouse MC38 syngeneic tumor model studies shown in figure 4 that while twice weekly administration of BT7480 could cause tumor eradication in 80%–100% of mice at modest doses (1.5–5 mg/kg), a weekly regimen could also deliver a substantive cure rate. Remarkably, we found that splitting the dose and administering it at 0 and 24 hours, followed by no further dosing until day 7, also afforded robust tumor elimination (figure 4E) and indeed tumor immunity (figure 4F). Modeling of the plasma drug levels in the context of functional potency found that BT7480 levels are almost certainly far below effective levels for most of the time between the weekly dosing cycles. While not addressing directly either tumor drug levels or the time course of drug occupancy at CD137 or Nectin-4, our data indicate that maintaining continuous high drug levels is not needed and offered no advantage. We found the same profile for the EphA2-targeted CD137 agonist, BCY12491, in our earlier report and therefore we suggest this is a general finding for CD137-driven tumor immunity.¹⁴ A feature of bispecific agents, including BT7480, is the hook effect phenomenon where at high concentrations

of drug both targets, in this case Nectin-4 and CD137, become independently saturated with drug, such that any activity that is dependent on co-ligation is progressively lost (figure 3). This has important ramifications in the clinical setting and could potentially lead to a bell-shaped dose response curve. This is interesting in mouse models but potentially of greater consequence in clinical development for agents with a long half-life. The relatively short half-life of BT7480 is thus potentially a discrete advantage as a drug in patients compared with biologicals because even if some degree of hook effect occurred it would dissipate relatively quickly.

The apparent sufficiency of a transient exposure to drug and an initial burst of CD137 agonism becomes even more credible in the light of the mechanistic data presented in figure 5. Analysis of NanoString mRNA profiling conducted on tumors excised at several times during the week following the 0 hour/24 hours treatment cycle revealed a two-step process. First and immediately, genes relating to myeloid cells (a macrophage score) and myeloid cell activation (a range of cytokine transcripts) increased for 2 days but returned to baseline within 4 days. Second, beginning between 2 and 4 days after administration of BT7480 and staying elevated, was a gene signature indicative of cytotoxic cell infiltration. This latter event was corroborated with IHC analysis revealing a profound CD8 + T cell infiltrate in the tumor at 6 days. We cannot discriminate between a direct action of BT7480 on resident myeloid cells versus a burst of myeloid activation secondary to activation of a small number of resident T cells, but the implications are the same. Specifically, that abundant T cell infiltrates may not be required for BT7480 to initiate tumor rejection which both broadens the potential number of patients that may benefit and indicates an orthogonal mechanism and therefore likely combination benefit with dominant immunotherapeutics such as PD-1 pathway blockers. Recent work by Litchfield and coworkers²⁶ identified expression of CXCL9, a myeloid-derived chemokine involved in recruitment of cytotoxic T cells,³³ as a strong predictor of response to checkpoint inhibitor therapy in a cohort of more than 1000 patients with cancer. We found robust upregulation of CXCL9 expression by BT7480 in our preclinical studies, supporting the translational relevance of our mechanistic findings.

We noted with interest, and showed in figure 5A, that the Nectin-4-expressing tumors that grew following subcutaneous implantation in mice were not uniformly positive for Nectin-4 on IHC staining. In fact, Nectin-4 expression was sparse. That BT7480 can readily and robustly cause tumor elimination despite this patchy expression of Nectin-4 is in fact consistent with the mechanism of action suggested by our tumor profiling data, specifically that BT7480 catalyzes a cascade of myeloid activation that drives extensive T cell infiltration. This proposed mechanism of action is in stark contrast and complimentary to the mechanism of action of Nectin-4-targeted chemotherapeutics such as enfortumab vedotin and BT8009 which cause tumor cell death.^{34 35} It is possible that those incoming T cells are then also subject to enhanced

activation and function due to direct action of BT7480, but it may not be necessary. Finally, the mechanistic analyses (figure 5) and blood gene expression profiling data reported here (figure 6) serve to enable a translational hypothesis for the measurement of the PD activity of BT7480 in patients with cancer that is suitable for deployment in a phase 1 clinical trial.

BT7480 is a first-in-class, chemically synthetic, targeted immune cell agonist advancing into clinical trials for treatment of Nectin-4-positive cancers. It is potent, specific, effective, and well tolerated in preclinical species and is therefore uniquely positioned to test the hypothesis in humans that intermittent CD137 agonism, potentially combined with chemotherapeutics and existing approved immunotherapies, can improve response rates and overall survival in cancer.

Acknowledgements The authors would like to thank Sarah Gattineri for editorial assistance, Laura Goodfield and Anna Licht for valuable discussions and technical assistance, and the research teams (past and present) at Bicycle Therapeutics for scientific contributions. We thank the teams at WuXi AppTec and CordenPharma for chemistry support, WuXi AppTec team for in vivo pharmacology support and Charles River Laboratories, Retrogenix, NeoGenomics, and Rancho Biosciences for support with several studies included in this report.

Contributors KH, JL, PU, EH, HC, ER, DK, JM, JK, FY, CC, DW, MK, SB, PJ, KM, and PB designed experiments; ER, DK, JM, and FY performed experiments; JL, PU, EH, HC, ER, DK, JM, JK, MK, and KM analyzed data; KH, JL, PU, EH, HC, KM, PB, and NK wrote the paper; KH, JL, PU, EH, HC, JK, CC, DW, MK, SB, PJ, KM, PB, and NK supervised research; KM and NK conceived of the project; NK is the guarantor of this work.

Funding This study was funded by Bicycle Therapeutics.

Competing interests All authors were full-time employees of Bicycle Therapeutics at the time that the work was conducted and some own stock or stock options in Bicycle Therapeutics. JL, PU, and KM are named on patent applications relating to compounds described in this work.

Patient consent for publication Not applicable.

Provenance and peer review Not commissioned; externally peer reviewed.

Data availability statement Data are available upon reasonable request.

Supplemental material This content has been supplied by the author(s). It has not been vetted by BMJ Publishing Group Limited (BMJ) and may not have been peer-reviewed. Any opinions or recommendations discussed are solely those of the author(s) and are not endorsed by BMJ. BMJ disclaims all liability and responsibility arising from any reliance placed on the content. Where the content includes any translated material, BMJ does not warrant the accuracy and reliability of the translations (including but not limited to local regulations, clinical guidelines, terminology, drug names and drug dosages), and is not responsible for any error and/or omissions arising from translation and adaptation or otherwise.

Open access This is an open access article distributed in accordance with the Creative Commons Attribution Non Commercial (CC BY-NC 4.0) license, which permits others to distribute, remix, adapt, build upon this work non-commercially, and license their derivative works on different terms, provided the original work is properly cited, appropriate credit is given, any changes made indicated, and the use is non-commercial. See <http://creativecommons.org/licenses/by-nc/4.0/>.

ORCID iD

Nicholas Keen <http://orcid.org/0000-0003-0741-3716>

REFERENCES

- 1 Chester C, Sanmamed MF, Wang J, *et al*. Immunotherapy targeting 4-1BB: mechanistic rationale, clinical results, and future strategies. *Blood* 2018;131:49–57.
- 2 Sanchez-Paulete AR, Labiano S, Rodriguez-Ruiz ME, *et al*. Deciphering CD137 (4-1BB) signaling in T-cell costimulation for

- translation into successful cancer immunotherapy. *Eur J Immunol* 2016;46:513–22.
- 3 Moran AE, Kovacovics-Bankowski M, Weinberg AD. The TNFRs OX40, 4-1BB, and CD40 as targets for cancer immunotherapy. *Curr Opin Immunol* 2013;25:230–7.
 - 4 Melero I, Shuford WW, Newby SA, et al. Monoclonal antibodies against the 4-1BB T-cell activation molecule eradicate established tumors. *Nat Med* 1997;3:682–5.
 - 5 Fisher TS, Kamperschroer C, Oliphant T, et al. Targeting of 4-1BB by monoclonal antibody PF-05082566 enhances T-cell function and promotes anti-tumor activity. *Cancer Immunol Immunother* 2012;61:1721–33.
 - 6 Segal NH, He AR, Doi T, et al. Phase I study of single-agent Utomilumab (PF-05082566), a 4-1BB/CD137 agonist, in patients with advanced cancer. *Clin Cancer Res* 2018;24:1816–23.
 - 7 Segal NH, Logan TF, Hodi FS, et al. Results from an integrated safety analysis of Urelumab, an agonist anti-CD137 monoclonal antibody. *Clin Cancer Res* 2017;23:1929–36.
 - 8 Etxeberria I, Glez-Vaz J, Teijeira Álvaro, et al. New emerging targets in cancer immunotherapy: CD137/4-1BB costimulatory axis. *ESMO Open* 2020;4:e000733.
 - 9 Claus C, Ferrara C, Xu W, et al. Tumor-targeted 4-1BB agonists for combination with T cell bispecific antibodies as off-the-shelf therapy. *Sci Transl Med* 2019;11:1. doi:10.1126/scitranslmed.aav5989
 - 10 Hinner MJ, Aiba RSB, Jaquin TJ, et al. Tumor-Localized costimulatory T-cell engagement by the 4-1BB/HER2 bispecific antibody-anticalin fusion PRS-343. *Clin Cancer Res* 2019;25:5878–89.
 - 11 Lakins MA, Koers A, Giambalvo R, et al. FS222, a CD137/PD-L1 tetravalent bispecific antibody, exhibits low toxicity and antitumor activity in colorectal cancer models. *Clin Cancer Res* 2020;26:4154–67.
 - 12 Ku G, Bendell JC, Tolcher AW, et al. 525O a phase I dose escalation study of PRS-343, a HER2/4-1BB bispecific molecule, in patients with HER2-positive malignancies. *Ann Oncol* 2020;31:S462–3.
 - 13 Melero I, Sanmamed MF, Calvo E, et al. 1025MO first-in-human (FIH) phase I study of RO7122290 (RO), a novel FAP-targeted 4-1BB agonist, administered as single agent and in combination with atezolizumab (ATZ) to patients with advanced solid tumours. *Ann Oncol* 2020;31:S707.
 - 14 Upadhyaya P, Lahdenranta J, Hurov K, et al. Anticancer immunity induced by a synthetic tumor-targeted CD137 agonist. *J Immunother Cancer* 2021;9:e001762.
 - 15 Samanta D, Almo SC. Nectin family of cell-adhesion molecules: structural and molecular aspects of function and specificity. *Cell Mol Life Sci* 2015;72:645–58.
 - 16 Challita-Eid PM, Satpayev D, Yang P, et al. Enfortumab vedotin antibody-drug conjugate targeting nectin-4 is a highly potent therapeutic agent in multiple preclinical cancer models. *Cancer Res* 2016;76:3003–13.
 - 17 M-Rabet M, Cabaud O, Josselin E, et al. Nectin-4: a new prognostic biomarker for efficient therapeutic targeting of primary and metastatic triple-negative breast cancer. *Ann Oncol* 2017;28:769–76.
 - 18 Takano A, Ishikawa N, Nishino R, et al. Identification of nectin-4 oncoprotein as a diagnostic and therapeutic target for lung cancer. *Cancer Res* 2009;69:6694–703.
 - 19 Nishiwada S, Sho M, Yasuda S, et al. Nectin-4 expression contributes to tumor proliferation, angiogenesis and patient prognosis in human pancreatic cancer. *J Exp Clin Cancer Res* 2015;34:30.
 - 20 Zhang Y, Zhang J, Shen Q, et al. High expression of Nectin-4 is associated with unfavorable prognosis in gastric cancer. *Oncol Lett* 2018;15:8789–95.
 - 21 Deng H, Shi H, Chen L, et al. Over-expression of Nectin-4 promotes progression of esophageal cancer and correlates with poor prognosis of the patients. *Cancer Cell Int* 2019;19:106.
 - 22 Rosenberg J, Sridhar SS, Zhang J, et al. EV-101: a phase I study of single-agent enfortumab vedotin in patients with Nectin-4-Positive solid tumors, including metastatic urothelial carcinoma. *J Clin Oncol* 2020;38:1041–9.
 - 23 Rosenberg JE, O'Donnell PH, Balar AV, et al. Pivotal trial of enfortumab vedotin in urothelial carcinoma after platinum and anti-programmed death 1/Programmed death ligand 1 therapy. *J Clin Oncol* 2019;37:2592–600.
 - 24 Freeth J, Soden J. New advances in cell microarray technology to expand applications in target deconvolution and off-target screening. *SLAS Discov* 2020;25:223–30.
 - 25 Douglass EF, Miller CJ, Sparer G, et al. A comprehensive mathematical model for three-body binding equilibria. *J Am Chem Soc* 2013;135:6092–9.
 - 26 Litchfield K, Reading JL, Puttick C, et al. Meta-analysis of tumor- and T cell-intrinsic mechanisms of sensitization to checkpoint inhibition. *Cell* 2021;184:596–614.
 - 27 Bartkowiak T, Jaiswal AR, Ager CR, et al. Activation of 4-1BB on liver myeloid cells triggers hepatitis via an Interleukin-27-Dependent pathway. *Clin Cancer Res* 2018;24:1138–51.
 - 28 Mayes PA, Hance KW, Hoos A. The promise and challenges of immune agonist antibody development in cancer. *Nat Rev Drug Discov* 2018;17:509–27.
 - 29 Eskiocak U, Guzman W, Wolf B, et al. Differentiated agonistic antibody targeting CD137 eradicates large tumors without hepatotoxicity. *JCI Insight* 2020;5 doi:10.1172/jci.insight.133647
 - 30 Qi X, Li F, Wu Y, et al. Optimization of 4-1BB antibody for cancer immunotherapy by balancing agonistic strength with FcγR affinity. *Nat Commun* 2019;10:2141.
 - 31 Kamata-Sakurai M, Narita Y, Hori Y, et al. Antibody to CD137 activated by extracellular adenosine triphosphate is tumor selective and broadly effective *In Vivo* without systemic immune activation. *Cancer Discov* 2021;11:158–75.
 - 32 You G, Lee Y, Kang Y-W, et al. B7-H3×4-1BB bispecific antibody augments antitumor immunity by enhancing terminally differentiated CD8⁺ tumor-infiltrating lymphocytes. *Sci Adv* 2021;7. doi:10.1126/sciadv.aax3160. [Epub ahead of print: 15 01 2021].
 - 33 Marcovecchio PM, Thomas G, Salek-Ardakani S. CXCL9-expressing tumor-associated macrophages: new players in the fight against cancer. *J Immunother Cancer* 2021;9:e002045.
 - 34 Liu BA, Olson D, Snead K, et al. Abstract 5581: Enfortumab vedotin, an anti-Nectin-4 ADC demonstrates bystander cell killing and immunogenic cell death anti-tumor activity mechanisms of action in urothelial cancers. *Cancer Research* 2020;80:5581.
 - 35 Rigby M, Bennett G, Chen L, et al. Abstract C061: BT8009, a bicycle toxin conjugate targeting Nectin-4, shows target selectivity, and efficacy in preclinical large and small tumor models. *Molecular Cancer Therapeutics* 2019;18:C061-C.